Estimation and Control for Collective Motion with Intermittent Locomotion

Anthony A. Thompson[1], Leela Cañuelas[2], Derek A. Paley[3]

***Abstract*— Inspired by the periodic swimming of many fish species, this paper presents a dynamic model of self-propelled particles with a periodic controller. The dynamics are split into a burst phase during which each particle applies a control input and a coast phase during which each particle performs state estimation. Using a closed-loop heading controller and a linear observer, we evaluate conditions that stabilize the equilibrium points for a single particle and for multiple particles using noise-free state feedback or output feedback. Practical stability bounds are evaluated for a single particle with bounded actuator noise with state feedback and bounded sensor noise with output feedback.**

I. Introduction

Biological species ranging from gray squirrels to zebrafish traverse their environments with discrete motions that alternate between perception and action [1]–[6]. For aquatic species like the zebrafish, this discrete behavior is hypothesized to be the result of perceptual degradation in their sensory organs due to self-generated motions like swimming [6]–[8]. The intermittent swimming behaviors of these biological fish offer many benefits including reduced cost of transport, enhanced functionality of sensory organs, improved localization in pursuit of prey, and ample time to process the perceived environment and formulate motor commands in response [1], [5], [7].

While the kinematic modeling of intermittent swimming in biological fish has received ample attention, the dynamic modeling of these behaviors in fish is not well studied. In [9], the energy-saving benefits of intermittent swimming was compared to continuous swimming for a self-propelled particle with optimal thrust inputs. In [10] and [11], computational fluid dynamics is used to examine the difference in hydrodynamic forces of intermittent and continuously swimming fish. Intermittent swimming is found to be more energy efficient than continuous swimming at high Reynolds numbers and with moderate values for the duty cycle between the burst and coast phases [10], [11]. In [12], the stability conditions of an intermittent consensus controller for a multi-agent system with nonlinear Euclidean dynamics are shown to depend on the dynamic coupling between the agents and their communication protocol.

To study the effects of separating estimation and control, we introduce a dynamic model of multiple self-propelled particles with non-overlapping actuation and sensing phases. The actuation phase applies thrust and steering control, whereas the sensing phase estimates the relative headings of other particles; in the single-particle case, the particle estimates its own heading. To analyze the stability of the heading dynamics, we integrate the continuous dynamics to obtain a discrete map and use Lyapunov's indirect method. We provide conditions on system parameters that guarantee exponential convergence to the equilibrium point using either state-feedback or output feedback for both the single-particle and multi-particle systems. In the presence of actuation

*This work was supported by ONR Grant No. 115239289.

[1]A. A. Thompson is a graduate research assistant in the Department of Aerospace Engineering, University of Maryland, College Park, MD, 20742, USA (e-mail: athomp95@umd.edu)

[2]L. Cañuelas is a undergraduate student in the Department of Physics, Brown University, Providence, RI, 02912, USA (e-mail: leela_canuelas-puri@brown.edu)

[3]D. A. Paley is the Willis H. Young Jr. Professor of Aerospace Engineering Education in the Department of Aerospace Engineering and the Institute for Systems Research, University of Maryland, College Park, MD, 20742, USA (e-mail: dpaley@umd.edu)

and measurement noise, we use Lyapunov's direct method to establish practical stability bounds for the desired equilibrium point of a single particle.

The contributions of this paper are (1) a dynamic model that describes intermittent behavior with non-overlapping sensing and actuation; (2) stability analysis, first of a single particle and then of a multi-particle system, with burst and coast dynamics and closed-loop heading control using either state or output feedback; (3) practical stability bounds for a single particle in the presence of bounded actuator and measurement noise. These results provide a fundamental understanding of the effects of separating estimation and control through intermittent locomotion in fish-inspired robots.

This paper is organized as follows. Section II reviews the dynamics of a self-propelled particle and a heading synchronization controller for multiple particles. Section III introduces the intermittent dynamics of a single particle and analyzes the stability conditions of the zero-noise state and output feedback cases. Section IV investigates the single-particle stability properties with bounded noise. Section V analyzes the stability conditions for multi-particle intermittent synchronization with noise-free state and output feedback. Section VI summarizes the paper and discusses ongoing and future work.

II. Background

This section presents a dynamic model for planar locomotion using self-propelled particles and a closed-loop heading synchronization controller for multiple self-propelled particles.

A. Modeling planar locomotion

We invoke the dynamics of a self-propelled particle to model the planar locomotion of a body in a fluid. The dynamics of a self-propelled particle are useful to describe motion that distinguishes between translational acceleration (thrust) and rotational acceleration (turning), accomplished by expressing the particle's velocity and control inputs in polar coordinates.

Let $r_n \in \mathbb{C}$ be the position of the nth particle in the complex plane such that $r_n = x_n + jy_n$, where $x_n, y_n \in \mathbb{R}$, j is the imaginary unit, and $n = 1,2,\ldots,N$. Let $\theta_n \in \mathbf{S}^1$ and $s_n \geq 0$ be the orientation and magnitude of the particle's velocity, respectively. The self-propelled particle dynamics are [13]

$$\begin{aligned} \dot{r}_n &= s_n e^{j\theta_n} \\ \dot{\theta}_n &= u_n \\ \dot{s}_n &= \nu_n, \end{aligned} \tag{1}$$

where u_n is the steering control and ν_n is the thrust control.

To steer the particle's velocity to a desired direction θ_d, consider the control input

$$u_n = K \sin(\theta_d - \theta_n), \tag{2}$$

where $K > 0$ is the control gain. The heading dynamics in (1) with control (2) has equilibrium points at $\theta^* = \theta_d$ and $\theta^* = \theta_d \pm \pi$. Linearization indicates that the only stable equilibrium point is $\theta^* = \theta_d$.

Model (1) will represent the burst and coast phases of the intermittent dynamic model, with (2) used for closed-loop steering control during the burst phase of a single particle. The multi-particle control law is introduced next.

B. Multi-particle Formation Control

Using (1) to model the dynamics of N particles with an all-to-all communication topology, the following controller synchronizes their headings into a parallel formation [14], [15]:

$$u_n = \frac{K}{N} \sum_{m=1}^{N} \sin(\theta_m - \theta_n), \ n = 1, \cdots, N. \tag{3}$$

The equilibrium points of the closed loop heading dynamics (1) with steering input (3) and constant velocity (i.e., $\nu_n = 0$) are classified as synchronized, balanced, and anti-parallel [14]. The synchronized equilibrium point is asymptotically stable if $K > 0$ and all other equilibrium points are unstable [14]. In Section V, (3) is used to synchronize the headings of multiple particles with synchronous cycles (i.e., aligned burst phases).

III. Single Particle Burst and Coast Dynamics

This section presents a dynamic model of burst and coast behavior in which sensing and actuation occur during non-overlapping phases.

A single burst phase combined with a single coast phase is called a cycle. Index $k = 0, 1, \ldots$ denotes the kth cycle. The duration of the burst and coast phases in a single cycle are denoted $\beta > 0$ and $T > 0$, respectively, and are identical for all k. The start time of cycle k is $t_k = k(\beta + T)$, where $t_0 = 0$.

A. Intermittent Dynamic Modeling

The dynamics during the burst phase are adapted from (1). First, assume that the steering and thrust inputs for the kth burst phase, i.e., $u(t) = u(t_k)$ and $\nu(t) = \nu(t_k)$, are constant for $t \in [t_k, t_k + \beta]$. The steering input u is subject to actuator noise ξ, whereas the particle's thrust is subject to quadratic drag with coefficient b. The burst dynamics for cycle k are

$$\dot{r} = se^{j\theta} \tag{4}$$
$$\dot{\theta} = u(t_k) + \xi \tag{5}$$
$$\dot{s} = -bs^2 + \nu(t_k). \tag{6}$$

The values $r(t_k)$, $\theta(t_k)$, and $s(t_k)$ at the start of the kth burst phase are equal to the values of the corresponding state variables at the conclusion of the previous coast phase for $k > 0$ and equal to the initial conditions for $k = 0$.

Since there is no actuation during the coast phase, the dynamics are equivalent to (4)–(6) with $u(t_k) = 0$, $\nu(t_k) = 0$, and $\xi = 0$. Observations collected during the coast phase are denoted by y and are equal to the (constant) orientation θ of the particle's velocity subject to sensor noise η. Let $\hat{\theta}$ denote the estimate of θ. The coast phase dynamics, including a linear observer for θ with observer gain L, are

$$\dot{r} = se^{j\theta} \tag{7}$$
$$\dot{\theta} = 0 \tag{8}$$
$$\dot{s} = -bs^2 \tag{9}$$
$$\dot{\hat{\theta}} = L(y - \hat{\theta}) \tag{10}$$
$$y = \theta + \eta. \tag{11}$$

The initial conditions for coast phase k are $r(t_k + \beta)$, $\theta(t_k + \beta)$, and $s(t_k + \beta)$. Furthermore, the initial heading estimate is $\hat{\theta}(t_k) = \hat{\theta}(t_{k-1})$ for $k > 0$ and $\hat{\theta}(t_k) = 0$ for $k = 0$. Figure 1 illustrates the dynamic model.

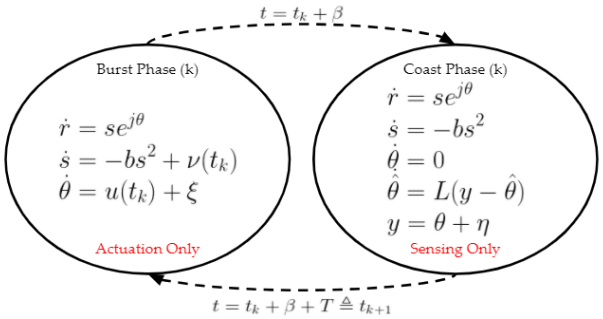

Fig. 1: Block diagram of the dynamic model with intermittent locomotion of a single particle. Actuation occurs during the burst phase and sensing occurs during the coast phase.

B. State Feedback Heading Dynamics

For state feedback, the controls u and ν are constant during the burst phase of each cycle. To track the desired heading θ_d, consider the steering control (2) evaluated at the start time t_k of burst phase k:

$$u(t_k) = K \sin(\theta_d - \theta(t_k)) \tag{12}$$

The thrust control during the burst phase is $\nu(t_k) = \nu_0$. This subsection characterizes the stability of the heading dynamics (5) with control (12) and no noise, i.e., $\xi = 0$; we consider the case $\xi \neq 0$ in Section IV.

The mapping from $\theta(t_k)$ to $\theta(t_{k+1})$ is obtained by substituting (12) into (5) and integrating from t_k to $t_k + \beta$ for the burst phase and integrating (8) from $t_k + \beta$ to $t_k + \beta + T = t_{k+1}$ for the coast phase. We obtain

$$\theta(t_{k+1}) = f(\theta(t_k)), \tag{13}$$

where

$$f(\theta) = \theta + K\beta \sin(\theta_d - \theta). \tag{14}$$

The equilibrium points θ^* of the map (13) are the solutions to the equation $\theta = f(\theta)$, i.e., $\theta^* = \theta_d$ and $\theta^* = \theta_d \pm \pi$. To evaluate the stability of θ^*, take the Jacobian of (14) and evaluate it at θ^*. For $\theta^* = \theta_d$, we have

$$\left.\frac{\partial f}{\partial \theta}\right|_{\theta^* = \theta_d} = 1 - K\beta. \tag{15}$$

The following theorem states the necessary and sufficient conditions on the control gain

K and burst duration β for $\theta^* = \theta_d$ to be an exponentially stable equilibrium point.

Theorem 1. *The map (14) corresponding to the closed-loop heading dynamics with noise-free state feedback exponentially stabilizes the equilibrium point $\theta^* = \theta_d$ if and only if $0 < K\beta < 2$. The equilibrium points $\theta^* = \theta_d \pm \pi$ are unstable.*

Proof. The proof follows from the stability condition for a map, which requires the eigenvalue(s) to lie within the unit circle. The map (13) is one dimensional and the sole eigenvalue at $\theta^* = \theta_d$ is given by (15). Evaluating $|1-K\beta| < 1$, i.e., $-1 < 1-K\beta < 1$, yields the desired result. The eigenvalue at $\theta^* = \theta_d \pm \pi$ is $1+K\beta$, which is always greater than one because K and β are positive. ■

C. Output Feedback Heading Dynamics

In the output-feedback case, θ is estimated using the linear observer (10) with observations (11). The intermittent behavior of a particle following these dynamics using output feedback is shown in Figure 2. The remainder of this subsection characterizes the stability of the heading dynamics (5) with noise-free output feedback, i.e., $\eta = 0$; we consider the case $\eta \neq 0$ in Section IV.

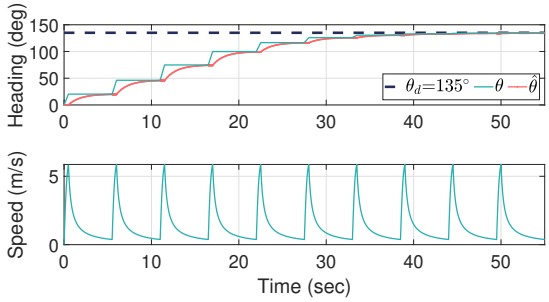

Fig. 2: Burst and coast behavior of a single particle using output feedback to steer in the desired direction $\theta_d = 135°$.

Since the output feedback control of θ utilizes the heading estimate $\hat{\theta}$, the closed-loop heading dynamics may be described using a two-dimensional map. Let $g(\theta,\hat{\theta})$ represent the map

$$(\theta(t_{k+1}),\hat{\theta}(t_{k+1})) = g(\theta(t_k),\hat{\theta}(t_k)), \qquad (16)$$

where $g_1(\theta,\hat{\theta})$ denotes the map from $\theta(t_k)$ and $\hat{\theta}(t_k)$ to $\theta(t_{k+1})$ and $g_2(\theta,\hat{\theta})$ denotes the map from $\theta(t_k)$ and $\hat{\theta}(t_k)$ to $\hat{\theta}(t_{k+1})$.

Since the heading estimate $\hat{\theta}(t_k)$ is constant during the burst phase, we have

$$u(t_k) = K\sin(\theta_d - \hat{\theta}(t_k)). \qquad (17)$$

The output feedback map is

$$g_1(\theta,\hat{\theta}) = \theta + K\beta\sin(\theta_d - \hat{\theta}). \qquad (18)$$

The map $g_2(\theta,\hat{\theta})$ is constructed by analyzing the burst and coast phases separately. Since the heading estimate is constant during the burst phase, $\hat{\theta}(t_k+\beta) = \hat{\theta}(t_k)$. During the coast phase, $\dot{\theta} = 0$, which implies $y = \theta$ is constant from $t_k + \beta$ to $t_k + \beta + T$. The map $\hat{\theta}(t_k+\beta)$ to $\hat{\theta}(t_{k+1})$ is obtained by integrating (10) with $\eta = 0$ to obtain

$$\hat{\theta}(t_{k+1}) = \theta(t_k+\beta)(1-e^{-LT}) + \hat{\theta}(t_k+\beta)e^{-LT}. \qquad (19)$$

Substituting $\theta(t_k+\beta) = g_1(\theta(t_k),\hat{\theta}(t_k))$ into (19) and using $\hat{\theta}(t_k+\beta) = \hat{\theta}(t_k)$ yields

$$g_2(\theta,\hat{\theta}) = (1-e^{-LT})(\theta + K\beta\sin(\theta_d - \hat{\theta})) + e^{-LT}\hat{\theta}. \qquad (20)$$

Let $z = [\theta,\hat{\theta}]^T$, which implies $z(t_{k+1}) = g(z(t_k))$, where g_1 and g_2 are given by (18) and (20), respectively. The equilibrium points of $g(z)$ are $z^* = (\theta^*,\theta^*)$, where $\theta^* = \theta_d$ or $\theta^* = \theta_d \pm \pi$. Linearizing $g(z)$ about $z^* = (\theta_d,\theta_d)$ yields the following two-dimensional linear map:

$$\frac{\partial g}{\partial z}\Big|_{z=z^*} = \begin{bmatrix} 1 & -K\beta \\ 1-e^{-LT} & K\beta\left(e^{-LT}-1\right)+e^{-LT} \end{bmatrix} \qquad (21)$$

The following theorem provides conditions on K, L, β and T that exponentially stabilize the equilibrium point $z^* = (\theta_d,\theta_d)$. The other equilibrium points are unstable. The proof invokes the stability triangle of a $2D$ map in its trace-determinant plane [16, p. 317].

Theorem 2. *The map $g(\theta,\hat{\theta})$ given by (18) and (20) corresponding to the closed-loop heading dynamics with noise-free output feedback exponentially stabilizes the equilibrium point $(\theta^*,\hat{\theta}^*) = (\theta_d,\theta_d)$ if and only if $LT > 0$ and $0 < K\beta < \frac{2(1+e^{-LT})}{1-e^{-LT}}$.*

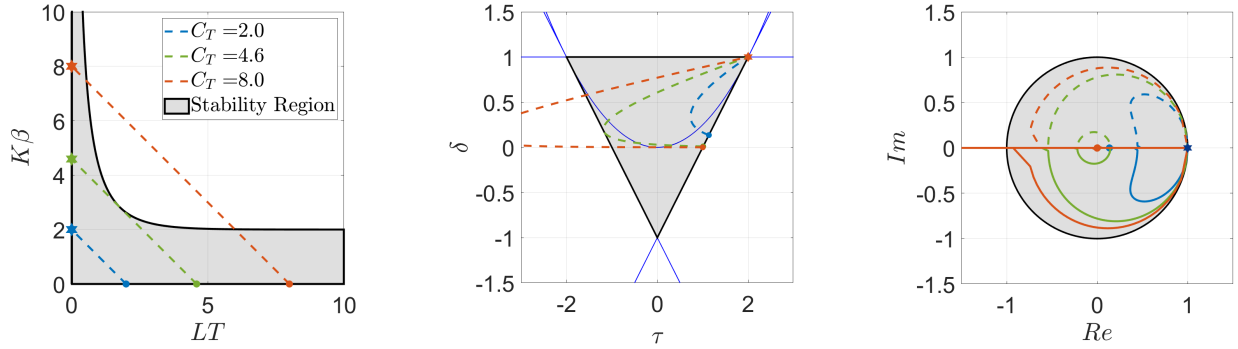

(a) $K\beta$-LT plane (b) trace-determinant plane (c) complex plane

Fig. 3: Stability regions of the burst and coast dynamics using noise-free output feedback with $K = L = 1$ and three values of the cycle time $C_T = \beta + T$. The shaded regions are stable

Proof. Let τ and δ be the trace and determinant of (21), respectively, such that

$$\tau = 1 + K\beta e^{-LT} - K\beta + e^{-LT} \quad (22)$$
$$\delta = e^{-LT}. \quad (23)$$

From [16], $\delta < 1$ is the first necessary condition for a stable $2D$ map. Substituting (23) into $\delta < 1$ and noting that $\delta > 0$, yields $0 < e^{-LT} < 1$, which implies the desired condition on the product LT. Substituting (22) and (23) into the second condition $\delta > -1 - \tau$ [16] yields $e^{-LT} > -2 - K\beta e^{-LT} + K\beta - e^{-LT}$, which implies

$$K\beta < \frac{2(1+e^{-LT})}{1-e^{-LT}}. \quad (24)$$

Substituting (22) and (23) into the third condition $\delta > -1 + \tau$ [16] yields $e^{-LT} > K\beta e^{-LT} - K\beta + e^{-LT}$, which implies $K\beta > 0$ as desired. ■

The results of Theorem 2 are illustrated in Figures 3a–3c. Certain values of $K\beta$, LT, and the overall cycle time $C_T = \beta + T$ can destabilize the desired equilibrium point. Figure 3a illustrates the stability region in the $K\beta$–LT plane with three values of C_T; Figure 3b illustrates the stability region in the trace-determinant plane; Figure 3c illustrates the stability region in the complex plane.

D. Bifurcations of Output Feedback Dynamics

This section analyzes bifurcations of the output feedback dynamics using the cycle time C_T as the bifurcation parameter. Solving for $\beta = C_T - T$ yields the following constraint on the trajectories in the $K\beta$–LT plane:

$$K\beta = K(C_T - T) = -\frac{K}{L}(LT) + KC_T, \quad (25)$$

corresponding to a line with slope $-\frac{K}{L}$ and vertical-axis intercept KC_T. The following corollary to Theorem 2 identifies the largest cycle time C_T for which all values of $K\beta$ and LT stabilize the desired equilibrium point $\theta^* = \theta_d$.

Corollary 1. *Consider the closed-loop heading dynamics with noise-free output feedback described in Theorem 2. Let $C_T = \beta + T$ denote the cycle time. The equilibrium point $\theta^* = \theta_d$ is exponentially stable for any control gain $K > 0$ and observer gain $L > 0$ if*

$$C_T < \frac{2(1+p)}{K(1-p)} + \frac{1}{L}\ln p \quad (26)$$

where

$$p = \frac{K + 2L + 2\sqrt{L(L+K)}}{K} \quad (27)$$

Proof. We seek a tangential intersection of the constraint (25) with the stability condition (24). An intersection occurs at the value of C_T for which (24) equals (25), which yields

$$C_T = \frac{2(1+e^{-LT})}{K(1-e^{-LT})} + \frac{1}{L}(LT). \quad (28)$$

The intersection is tangential if the derivatives of (24) and (25) are equal at the intersection point, i.e.,

$$-\frac{K}{L} = -\frac{4e^{-LT}}{(1-e^{-LT})^2}. \quad (29)$$

Equation (29) yields the following quadratic equation in terms of $p = e^{-LT}$:

$$Kp^2 - 2(K+2L)p + K = 0, \tag{30}$$

Solving for p using the quadratic equation and adopting the positive root gives the desired result. (The negative root does not satisfy the stability conditions in Theorem 2.) ■

IV. Noisy Sensing & Actuation

This section considers the robustness of the estimation and control results from Section III under the influence of sensor and actuator noise for a single particle. First, Lyapunov's direct method shows that $\theta^* = \theta_d$ is uniformly ultimately bounded under the dynamics (5) with state-feedback heading control (12) and actuator noise $\xi \neq 0$. Secondly, a similar analysis shows that the estimation error $\sigma = \theta - \hat{\theta}$ is uniformly ultimately bounded under the observer dynamics (10) with observation (11) and $\eta \neq 0$.

A. State Feedback Noisy Heading Control

Consider the heading dynamics (5) with state-feedback control (12) and bounded actuator noise ξ. Let $q = \theta - \theta_d$ denote the smallest angular difference between θ and θ_d. The map from $q(t_k)$ to $q(t_{k+1})$ is obtained from $f(\theta)$ in (14) by including $\bar{\xi} = \int_{t_k}^{t_{k+\beta}} \xi dt$ on the right-hand side and subtracting θ_d from both sides. Assume $|\bar{\xi}| \leq \gamma$. Taking the Taylor series expansion of $\sin q$ about $q = 0$ yields

$$q(t_{k+1}) = q(t_k) - K\beta q(t_k) + \bar{\xi}. \tag{31}$$

Consider a quadratic Lyapunov function candidate $V(q) = \frac{1}{2}q^2$. Let $\Delta V(t_k) = V(t_{k+1}) - V(t_k)$. Along solutions of the map (31), we have

$$\begin{aligned} \Delta V &= \tfrac{1}{2}K\beta(K\beta-2)q^2 + (1-K\beta)q\bar{\xi} + \tfrac{1}{2}\bar{\xi}^2 \\ &\leq \tfrac{1}{2}K\beta(K\beta-2)q^2 + |1-K\beta||q|\gamma + \tfrac{1}{2}\gamma^2 \end{aligned} \tag{32}$$

The following corollary to Theorem 1 identifies a bound on q proportional to the actuator noise bound γ.

Corollary 2. *Consider the closed-loop heading dynamics with noisy state feedback $\xi \neq 0$. Let $\bar{\xi} = \int_{t_k}^{t_k+\beta} \xi dt$ for all k. Assume $0 < K\beta < 2$, and $|\bar{\xi}| < \gamma$. The equilibrium point $\theta^* = \theta_d$ is uniformly ultimately bounded with bound $\frac{\gamma}{K\beta}$.*

Proof. Since $0 < KB < 2$, (32) corresponds to a concave-down parabola $\Delta V(z)$. Therefore, $V(z)$ is decreasing for all values of z for which $\Delta V < 0$. The roots $\Delta V = 0$ occur for $z = \frac{\gamma}{K\beta}$, which implies solutions converge to $|z| < \frac{\gamma}{K\beta}$. ■

B. Output Feedback with Noisy Measurements

Consider the observer dynamics (10) and measurement equation (11). Let η be bounded measurement noise satisfying $|\eta| < \Gamma$. The estimation error σ denotes the angular difference between θ and $\hat{\theta}$ during the coast phase. Since $\theta, \hat{\theta} \in S^1$, $\sigma = \theta - \hat{\theta}$ corresponds to the small angle between $e^{i\theta}$ and $e^{i\hat{\theta}}$. Since θ is constant during the coast phase, the time derivative of σ in the interval $t_k + \beta$ to $t_k + \beta + T$ is

$$\dot{\sigma} = -\dot{\hat{\theta}} = -L(\sigma + \eta). \tag{33}$$

Consider the quadratic Lyapunov function candidate $U(\sigma) = \frac{1}{2}\sigma^2$. The time-derivative of $U(\sigma)$ along solutions of (33) is

$$\dot{U} = -L\sigma^2 - L\eta\sigma. \tag{34}$$

The following corollary to Theorem 2 identifies a bound on σ equal to the sensor-noise bound.

Corollary 3. *Consider the observer dynamics (10) with $L > 0$ and bounded sensor noise $|\eta| < \Gamma$. The estimation error $\sigma = \theta - \hat{\theta}$ converges to $|\sigma| < \Gamma$.*

Proof. Since $|\eta| < \Gamma$, (34) becomes

$$\dot{U} \leq -L\sigma^2 + L\Gamma|\sigma|. \tag{35}$$

Therefore, U is decreasing outside of the region given by the non-zero roots of (35), i.e., $\sigma = \pm\Gamma$. ■

V. Multi-particle Synchronization

This section extends the intermittent dynamics to N particles with all-to-all communication and synchronous cycles. We adopt the intermittent dynamics from Section III and use subscript n to denote the nth particle. First, we introduce the heading consensus controller (3) used to align each particle's heading. Second, we examine the equilibrium points of the multi-particle system and determine the stability properties for the state feedback case. Third,

we devise an idealized sensor to observe the relative headings between each particle and determine the stability properties for the output feedback case.

A. State Feedback Heading Synchronization

As in the single-particle case, the constant thrust control input is $\nu_n = \nu_0$, but for multiple particles the constant steering input is [14]

$$u_n(t_k) = \frac{K}{N}\sum_{m=1}^{N}\sin\big(\theta_m(t_k)-\theta_n(t_k)\big), \tag{36}$$

which aligns each particle's heading (see Figure 4). The remainder of this section characterizes the stability of the heading dynamics (5) with (36) and no noise i.e., $\xi_n = 0$. Let $\boldsymbol{\theta}$ denote the vector of headings and h_n denote the map of the n^{th} particle's heading from $\theta_n(t_k)$ to $\theta_n(t_{k+1})$ such that $\theta_n(t_{k+1}) = h_n(\boldsymbol{\theta}(t_k))$, where h_n is

$$h_n(\boldsymbol{\theta}) = \theta_n + \frac{K\beta}{N}\sum_{m=1}^{N}\sin(\theta_m-\theta_n). \tag{37}$$

The synchronized equilibrium points of (37)

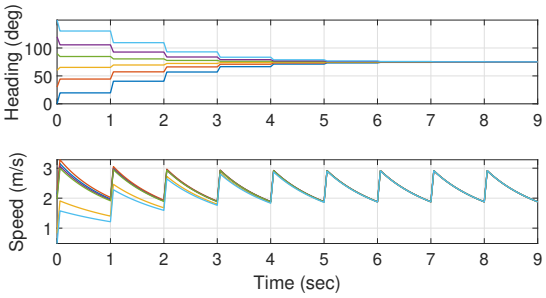

Fig. 4: Synchronization of multiple particles using intermittent state feedback heading control.

are $\boldsymbol{\theta}^* = \alpha\mathbb{1}$, where $\alpha \in \boldsymbol{S}^1$ and $\mathbb{1} = [1,\cdots,1]^T$. Linearizing (37) about $\boldsymbol{\theta}^*$ yields the $N\times N$ Jacobian matrix

$$\frac{\partial h_n}{\partial \boldsymbol{\theta}}\Big|_{\boldsymbol{\theta}=\boldsymbol{\theta}^*} = \begin{cases} 1-\dfrac{K\beta}{N}(N-1) & n=m \\ \dfrac{K\beta}{N} & n\neq m \end{cases}. \tag{38}$$

The eigenvalues of (38) are $\lambda = 1$ and $N-1$ repeated roots of $\lambda = 1-K\beta$. The eigenvector for the $\lambda = 1$ eigenvalue corresponds to the inertial frame's rotational symmetry and does not affect the convergence to $\boldsymbol{\theta}^*$. The following proposition provides conditions on $K\beta$ for $\boldsymbol{\theta}^* = \alpha\mathbb{1}$ to be exponentially stable. Note that the result is identical to the single-particle case.

Proposition 1. *The map* (37) *corresponding to the multi-particle closed-loop heading dynamics with noise-free state feedback exponentially stabilizes the synchronized equilibrium point if and only if* $0 < K\beta < 2$.

B. Output Feedback Heading Synchronization

Let the relative headings between the mth and nth particles be denoted as $\theta_{m,n} = \theta_m - \theta_n$, and let $\boldsymbol{\Delta\theta} = [\theta_{1,2},\cdots,\theta_{N,N-1}]^T$ be the N^2-N vector of relative headings for N particles. The output equation and linear observer dynamics for the multi-particle coast phase are

$$\boldsymbol{y} = \boldsymbol{\Delta\theta} + \boldsymbol{\eta} \tag{39}$$

and

$$\dot{\boldsymbol{\Delta\hat{\theta}}} = L\left(\boldsymbol{y} - \boldsymbol{\Delta\hat{\theta}}\right), \tag{40}$$

respectively, where L is the observer gain and $\boldsymbol{\Delta\hat{\theta}}$ is the vector of estimated relative headings.

We use an idealized sensor to estimate the relative headings during the coast phase. The estimated relative headings are used in the steering control input during the burst phase. The heading controller during the burst phase is

$$u_n = \frac{K}{N}\sum_{m=1}^{N}\sin(\hat{\theta}_{m,n}(t_k)). \tag{41}$$

Since (41) utilizes $\hat{\theta}_{m,n}(t_k)$, the closed-loop heading dynamics may be described using a N^2-dimensional map. Let $H(\boldsymbol{\theta},\boldsymbol{\Delta\hat{\theta}})$ represent the map so that

$$(\boldsymbol{\theta}(t_{k+1}),\boldsymbol{\hat{\theta}}(t_{k+1})) = H(\boldsymbol{\theta}(t_k),\boldsymbol{\Delta\hat{\theta}}(t_k)), \tag{42}$$

where $H_\theta(\boldsymbol{\theta},\boldsymbol{\Delta\hat{\theta}})$ denotes the map from $\theta_n(t_k)$ and $\boldsymbol{\Delta\hat{\theta}}_n(t_k)$ to $\theta_n(t_{k+1})$ and $H_{\Delta\theta}(\boldsymbol{\theta},\boldsymbol{\Delta\hat{\theta}})$ denotes the map from $\theta_n(t_k)$ and $\boldsymbol{\Delta\hat{\theta}}_n(t_k)$ to $\boldsymbol{\Delta\hat{\theta}}_n(t_{k+1})$.

The nth term of the multi-particle output feedback map is

$$H^n_\theta(\boldsymbol{\theta},\boldsymbol{\Delta\hat{\theta}}) = \theta_n + \frac{K\beta}{N}\sum_{m=1}^{N}\sin\left(\hat{\theta}_{m,n}\right). \tag{43}$$

The map $H_{\Delta\theta}(\boldsymbol{\theta},\boldsymbol{\Delta\hat{\theta}})$ is determined by integrating (40), substituting (43), and using $\theta_{m,n}(t_k+$

$\beta) = \theta_{m,n}(t_{k+1})$, which yields the (m,n)th term of

$$H^{m,n}_{\Delta\theta}(\boldsymbol{\theta}, \hat{\boldsymbol{\theta}}) = (1 - e^{-LT})\left(\theta_{m,n} + u_m - u_n\right) + e^{-LT}\hat{\theta}_{m,n}, \quad (44)$$

where u_m and u_n are given by (41) for the mth and nth particles, respectively.

Let $\boldsymbol{\phi} = [\boldsymbol{\theta}, \boldsymbol{\Delta}\hat{\boldsymbol{\theta}}]^T$ represent the N^2-dimensional column vector of the absolute headings and estimated relative headings. This implies that $\boldsymbol{\phi}(t_{k+1}) = H(\boldsymbol{\phi}(t_k))$, where H_θ and $H_{\Delta\theta}$ are given by (43) and (44), respectively. The synchronized equilibrium points of $H(\boldsymbol{\phi})$ are $\boldsymbol{\phi}^* = (\boldsymbol{\theta}^*, \boldsymbol{\Delta}\hat{\boldsymbol{\theta}}^*)$, where $\boldsymbol{\theta}^* = \alpha\mathbb{1}$ and $\boldsymbol{\Delta}\hat{\boldsymbol{\theta}}^* = \mathbf{0}$.

The following proposition provides conditions on the products $K\beta$ and LT that exponentially stabilize $\boldsymbol{\phi}^*$ for multiple particles. The other equilibrium points are unstable [14]. The proof for Proposition 2 is omitted due to the page constraints. Note, this result is identical to Theorem 2.

Proposition 2. *The map $H(\boldsymbol{\theta}, \boldsymbol{\Delta}\hat{\boldsymbol{\theta}})$ given by* (43) *and* (44) *corresponding to the closed-loop heading dynamics with noise-free output feedback exponentially stabilizes the synchronized equilibrium point if and only if $LT > 0$ and $0 < K\beta < \frac{2(1+e^{-LT})}{1-e^{-LT}}$.*

VI. Conclusion

This paper presents a bio-inspired dynamic model of planar self-propelled particles with intermittent heading sensing and control. Stability analysis of the noise-free state feedback and output feedback control provides conditions on control and observer gains to ensure exponential convergence of the equilibrium point in both the single and multi-particle cases. The heading estimation and control is robust to bounded measurement and actuation noise, respectively. Ongoing and future work seeks to expand this analysis to consider multiple particles with asynchronous cycles and actuator and sensor noise.

References

[1] A. P. Soto and M. J. McHenry, "Pursuit predation with intermittent locomotion in zebrafish," *J. of Experimental Biology*, vol. 223, no. 24, 2020.

[2] S. Bazazi, F. Bartumeus, J. J. Hale, and I. D. Couzin, "Intermittent motion in desert locusts: behavioural complexity in simple environments," *PLoS Comput Biol*, vol. 8, no. 5, p. e1002498, 2012.

[3] D. L. Kramer and R. L. McLaughlin, "The behavioral ecology of intermittent locomotion," *American Zoologist*, vol. 41, no. 2, pp. 137–153, 2001.

[4] E. J. Buskey, C. Coulter, and S. Strom, "Locomotory patterns of microzooplankton: potential effects on food selectivity of larval fish," *Bulletin of Marine Science*, vol. 53, no. 1, pp. 29–43, 1993.

[5] M. J. McHenry and G. V. Lauder, "The mechanical scaling of coasting in zebrafish (*Danio rerio*)," *J. of Experimental Biology*, vol. 208, no. 12, pp. 2289–2301, 2005.

[6] A. McKee, A. P. Soto, P. Chen, and M. J. McHenry, "The sensory basis of schooling by intermittent swimming in the rummy-nose tetra (*Hemigrammus rhodostomus*)," *Proceedings of the Royal Society B*, vol. 287, no. 1937, p. 20200568, 2020.

[7] E. T. Lunsford, D. A. Skandalis, and J. C. Liao, "Efferent modulation of spontaneous lateral line activity during and after zebrafish motor commands," *J. of Neurophysiology*, vol. 122, no. 6, pp. 2438–2448, 2019.

[8] K. E. Feitl, V. Ngo, and M. J. McHenry, "Are fish less responsive to a flow stimulus when swimming?" *J. of Experimental Biology*, vol. 213, no. 18, pp. 3131–3137, 2010.

[9] P. Paoletti and L. Mahadevan, "Intermittent locomotion as an optimal control strategy," *Proceedings of the Royal Society A: Mathematical, Physical and Engineering Sciences*, vol. 470, no. 2164, p. 20130535, 2014.

[10] M. Chung, "On burst-and-coast swimming performance in fish-like locomotion," *Bioinspiration & biomimetics*, vol. 4, no. 3, p. 036001, 2009.

[11] L. Dai, G. He, X. Zhang, and X. Zhang, "Intermittent locomotion of a fish-like swimmer driven by passive elastic mechanism," *Bioinspiration & biomimetics*, vol. 13, no. 5, p. 056011, 2018.

[12] A. Hu, J. H. Park, and M. Hu, "Consensus of nonlinear multiagent systems with intermittent dynamic event-triggered protocols," *Nonlinear Dynamics*, vol. 104, no. 2, pp. 1299–1313, 2021.

[13] E. W. Justh and P. Krishnaprasad, "Equilibria and steering laws for planar formations," *Systems & Control Letters*, vol. 52, no. 1, pp. 25–38, 2004.

[14] R. Sepulchre, D. A. Paley, and N. E. Leonard, "Stabilization of planar collective motion: All-to-all communication," *IEEE Transactions on Automatic Control*, vol. 52, no. 5, pp. 811–824, 2007.

[15] L. Scardovi, A. Sarlette, and R. Sepulchre, "Synchronization and balancing on the n-torus," *Systems & Control Letters*, vol. 56, no. 5, pp. 335–341, 2007.

[16] G.-I. Bischi, C. Chiarella, M. Kopel, F. Szidarovszky *et al.*, *Nonlinear oligopolies*. Springer, 2010.